Chemical Papers (2020) 74:4355–4363
https://doi.org/10.1007/s11696-020-01239-6

ORIGINAL PAPER

The influence of physical factors on the halochromic behavior of the pH-sensitive sulfonphthaleine dyes: a DFT study

Maryam Mojbafan[1] · Farzaneh Zanjanchi[1] · Mahboubeh Taherkhani[1]

Received: 17 February 2020 / Accepted: 30 May 2020 / Published online: 15 June 2020
© Institute of Chemistry, Slovak Academy of Sciences 2020

Abstract

Sulfonphthaleine dyes are important class of pH indicators with some applications in novel sensors. In this paper, the authors present a theoretical study to elucidate the effect of physical factors on the halochromic behavior of the sulfonphthaleine dyes. The studied sulfonphthaleine dyes are phenol red, cresol red, bromophenol blue and the physical factors such as temperature, pressure, dielectric constant of solvent and isotope type of constituent atoms are taken into account. In the meantime, changes of pH of the color change of the indicators, ΔpH, with the physical factors in the acid–base equilibrium of the indicators are studied. To this end, Enthalpy change, ΔH_a, entropy change, ΔS_a, Gibbs free energy change, ΔG_a, and equilibrium constant of ionization process of indicators, K_a, are calculated for the equilibrium reaction under different conditions; then their values are interpreted by the laws of thermodynamics and statistical thermodynamics. The results show that ΔpH is positive by increasing temperature at any pressure, increasing pressure at any temperature, decreasing the polarity of the solvent used, and using isotopes of constituent atoms. The effect of temperature and pressure on ΔpH is lower respectively under higher temperatures and pressures, and it is not dependent on the indicator type. The ΔpH values due to the isotopic factor depend on the type of atom as well as that of the indicator. These findings indicate the importance of physical factors on the halochromic behavior of dyes for further research and the development of pH-sensitive sensors.

Keywords DFT · Halochromic · pH indicator · Sulfonphthaleine dyes · Physical factors

Introduction

Chromism has become a booming research field in various scientific domains (Bamfield 2001; Golchoubian et al. 2019; Van der Schueren et al. 2012). Some dyes show chromic properties, which means that their color changes depending on external influences such as thermochromism, photochromism and halochromism properties. (Bamfield 2001; Barachevskii et al. 2012; De Meyer et al. 2014; Kim 2006; Kulinich and Ishchenko 2019; Kulinich et al. 2018; Surati and Shah 2015; Zollinger 2003). A halochromic material is a material whose color changes, when pH changes occur. The pH indicators have this property. To this day, the halochromic behavior of many dyes (azo, sulfonphthaleine, phenolphthalein, phenolate, quinolone dyes, etc.) has been studied experimentally and theoretically (De Meyer et al. 2014, 2016; Ghanadzadeh Gilani et al. 2017; Hermosilla et al. 2017; Hosseini et al. 2014; Van der Schueren et al. 2012; Zhang et al. 2009), but so far, and to the knowledge of the authors, the theoretical study of the effect of physical factors on the color change pH of the sulfonphthaleine dyes has not been done. In this research, we focus on three types of sulfonphthaleine dyes including phenol red, cresol red, and bromophenol blue. Sulfonphthaleine dyes form a relatively small dye class, but are widely used as acid–base indicators because they show a clear color transition in function of pH. Therefore, they find application in various other areas, such as detection of pesticides, acid vapours, ammonia, CO_2, the quantitation of proteins in solution, the textile sensor, the development of new glassy carbon electrodes and wound bandages (Chang et al. 2011; Chen et al. 2005; Clayton and Byrne 1993; De Meyer et al. 2016; Ensafi et al. 2010; Flores 1978; Hua et al. 2013; Kurzweilová and Sigler 1993; Nakamura and Amao 2003; Yang et al. 2010).

The basic structure of sulfonphthaleine dyes and substituents of the studied molecules are given in Fig. 1. The dye set in this work covers most commercially available

✉ Farzaneh Zanjanchi
fzanjanchi@yahoo.com

[1] Department of Chemistry, Takestan Branch, Islamic Azad University, Takestan, Iran

	R_1	R_2	R_3
phenol red	H	H	H
crosel red	CH_3	H	H
bromophenol blue	Br	Br	H

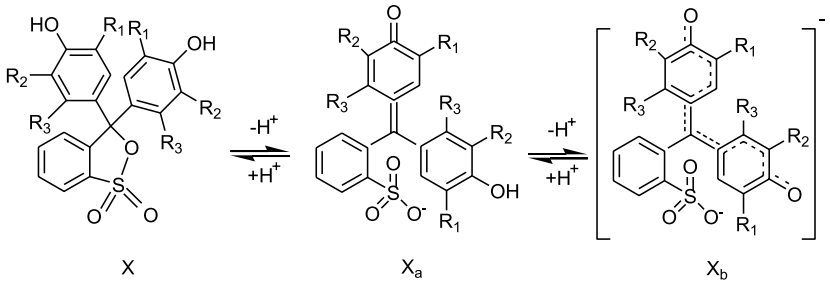

Fig. 1 Basic structure of sulfonphthaleine dyes, substituents of the studied molecules and general color changing mechanism for sulfonphthaleine dyes. While the neutral structure X is observed only in very acidic solutions or in powder, the relevant color change originates from a deprotonation from the single anionic form, X_a, to a double anion, X_b (De Meyer et al. 2014)

sulfonphthaleine compounds. These products have numerous applications, often in biological and medical fields (Byrne and Breland 1989; De Meyer et al. 2014; Flores 1978; Marona and Schapoval 2001; Yao and Byrne 2001). The color changing mechanism of sulfonphthaleine dyes can be ascribed to a protonation/deprotonation reaction, as illustrated in Fig. 1. The dyes can exist in a neutral form, X, in powder or in very acidic media. The most interesting molecular change (and thus color change), however, is the deprotonation of a single anion, X_a, to a resonance stabilized double anion, X_b. When it solvated, deprotonation will allow for a rearrangement of the internal bonds. The driving force behind this deprotonation is twofold: the internal rearrangement results in a larger conjugated system and a SO_3 group is formed. The latter allows for a high interaction with the surrounding solvent molecules and is thus energetically favorable. This internal rearrangement can be confirmed experimentally by drop in pH upon solvation and theoretically (a molecular dynamic simulation with explicit solvent) by drop in calculated Gibbs free energy (De Meyer et al. 2014). Therefore, in this study, only the equilibrium of single anion, X_a, and double anion, X_b, forms are considered to investigate the changes in the behavior of halochromic dyes with physical agents.

Since pH monitoring is one of the most important parameters in many industrial processes such as food, pharmaceutical, water and wastewater therefore, continuous online pH control and maintaining a proper pH range is essential in many of the physical and chemical reactions. pH variation can be affected on product quality and efficiency of chemical reactions. pH determination can be performed by using different methods. For example, pH test paper strips, electrochemical and photochemical sensors, etc. Although the pH test paper strips are available and easy to use, they are not used in high accuracy applications. In recent years, development of electrochemical and optical sensors has been a great interest that indicates the importance of this field in various sciences (Hosseini et al. 2014; Kelly and Cochrane 2015; Matějec et al. 2019; Steyaert et al. 2015; Sun et al. 2015). This research aims at theoretical and computational study of changes of pH indicators ranges (used in pH optical sensor) by physical factors of temperature, pressure, ionic strength of solvent, substituent groups and isotopic type of constituent atoms. The measure of the acid concentration in an organic media is a common issue in chemistry (Mineo et al. 2019). With the aim to study this subject in a facile and widely way, the halochromic properties of indicators in solvents with different dielectric constant are calculated. The importance and prevalence of isotopic types studies provide an incentive for development of new methods that can be used for rapid and selective detection and monitoring of the isotopic types both in the gaseous and in the liquid phases. Some traditional detection methods such as electrolysis, laser, NMR and MS spectroscopic techniques are usually employed for isotope sensing and detection; however, these methods are believed to be expensive and time consuming. The many uses of indicator or sensors of this type include monitoring air quality, indicating agricultural regime (nitrogen isotope relationships between crops and fertilizer), detecting volatile organic compounds, detecting toxic gases and controlling fossil fuel combustion products (Bateman et al. 2005; Gibson et al. 2012; Mineo et al. 2019; Özyiğitoğlu 2020).

The results of this research can be used in the design of favorable indicators and suitable and predictable conditions for implementation and synthesis of pH-sensitive sensors. Furthermore, the methodology of this work is applicable to other dye classes as well.

Materials and methods

In this study, all calculations on the structures of three types of indicators including phenol red, cresol red, and bromophenol blue, in modes of single anionic (acidic form) and a double anion (base form) were carried out in Gaussian03 using Density Functional Theory. Geometries were fully optimized using B3LYP/6-31G** level of theory (Frisch

et al. 2004). The optimized molecular structures of indicators in various forms are displayed in Fig. 2. Vibrational frequency calculations were performed at the same level of theory on the optimized structures to ensure the stability of structures and to calculate thermodynamic quantities. In acidic form, substituent element of hydroxyl in all dyes is protonated and deprotonated in basic form. The results of vibrational frequencies calculations indicate that all the studied structures contain real vibrational frequencies or number of zero negative imaginary frequency (NIMAG = 0).

The purpose of this research is to investigate the effect of physical factors on pH range of color change of indicators; therefore, all thermodynamic studies were done under different conditions of temperature (273.15, 298.15, 323.15 and 373.15 K), pressure (1, 5 and 10 atm), different phases (vacuum, benzene and water) and change of the isotopic type of carbon, oxygen and hydrogen atoms of the studied indicators ($^{12}C \rightarrow {}^{13}C$, $^{16}O \rightarrow {}^{18}O$ and $^{1}H \rightarrow {}^{2}H$).

In this study, Conductor—like Polarizable Continuum Model (CPCM) is used to consider the effect of solvent. The CPCM model was spread in the scientific community due to its accuracy and the relative simplicity of the expressions involved in the definition of the solvent reaction field. First and second derivatives of the molecular free energy with respect to nuclear motions needed for geometry optimizations and frequency calculations can be computed with accurate and very efficient algorithms. In this model, the solvent is considered as a continuous environment with a uniform dielectric constant inside which the soluble remains as a spherical cavity. Molecule polarity can create bipolarity in the environment, and the electric field created by solvent polarity can interact with the soluble molecule bipolarity which results in system stability (Cossi et al. 2003; Tomasi and Persico 1994).

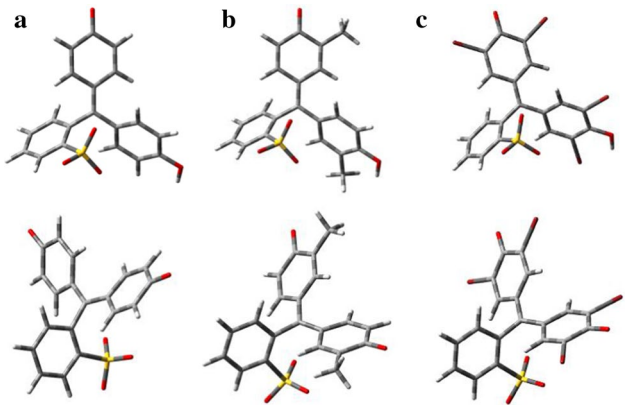

Fig. 2 The optimized molecular structures of **a** phenol red, **b** cresol red and **c** bromophenol blue indicators in the forms of 1) single anion, X_a, and 2) double anion, X_b, obtained at the B3LYP/6-31G** level of theory

Results and discussion

In the equilibrium reaction (Eq. 1), the equilibrium constant between the acid and the base states of indicators, K_a, and the relationship between equilibrium constant and Gibbs free energy change for the desired equilibrium, ΔG_a, are written as follows:

$$\mathrm{HIn} \Leftrightarrow \mathrm{H^+} + \mathrm{In^-} \tag{1}$$

$$K_a = \frac{[\mathrm{H^+}] \times [\mathrm{In^-}]}{[\mathrm{HIn}]} \tag{2}$$

$$\Delta G_a = -RT \ln(K_a) \tag{3}$$

Enthalpy change, ΔH_a, entropy change, ΔS_a, Gibbs free energy change, ΔG_a, and equilibrium constant of ionization process of indicator, K_a, are calculated for the equilibrium reaction (Eq. 1) under different conditions and are reported in Tables 1, 2 and 3.

The reported results in Tables 1, 2 and 3 show that ΔH_a is positive in all conditions which means the ionization process of indicators is endothermic. As the temperature increases under constant pressure, ΔH_a increases, and it remains constant under constant temperature by increasing the pressure; that is, ΔH_a does not depend on pressure. Since the enthalpy of ideal gases is pressure independent ($(\partial H/\partial P)_T = 0$) and in all calculations, reaction components are considered ideal gases; so the enthalpy changes of the reaction are independent of pressure. Ionization processes of indicators are less endothermic in dissolved state. ΔH_a decreases by increasing the solvents polarity (in water, ΔH_a is less than ethanol, and in ethanol, it is less than vacuum). ΔH_a increases by considering isotopic effect of constituent atoms in all cases. $T\Delta S_a$ is positive in all the studied conditions. Considering the fact that the number of process components in products is higher than raw materials, such conclusion is logical and correct. $T\Delta S_a$ increases by increasing the temperature under constant pressure and it decreases by increasing the pressure under constant temperature. By paying attention to thermodynamic relationships of $(\partial S/\partial P)_T = -\alpha V$ and $\alpha = 1/V(\partial V/\partial T)_P$ that α for ideal gases equals to $\alpha = 1/T$ is resulted $(\partial \Delta S/\partial P)_T = -\Delta V/T$ that ΔV and T both are positive quantities, therefore, ΔS must be decreased by increasing pressure under constant temperature. ΔG_a is positive in all conditions which means ionization process of indicators is non-spontaneous. Results show that ΔG_a decreases by increasing temperature under constant pressure and it increases by increasing pressure at constant temperature. Therefore, it is concluded that high temperature and low pressure conditions are favorable for the

Table 1 Thermodynamic quantities ΔH_a, $T\Delta S_a$ and ΔG_a in kcal/mol and equilibrium constants, K_a, for the indicators dissociation equilibrium of phenol red, cresol red and bromophenol blue in the gas phase and the different pressures and temperatures, respectively in K and atm obtained at the B3LYP/6-31G** level of theory

		Phenol red				Cresol red				Bromophenol blue			
P	T	ΔH_a	$T\Delta S_a$	ΔG_a	K_a	ΔH_a	$T\Delta S_a$	ΔG_a	K_a	ΔH_a	$T\Delta S_a$	ΔG_a	K_a
1	273.15	385.692	6.802	378.890	exp(− 698.1)	385.240	7.953	377.287	exp(− 695.1)	369.599	7.408	362.191	exp(− 667.3)
1	298.15	385.771	7.508	378.263	exp(− 638.5)	384.653	8.037	376.617	exp(− 635.7)	369.692	8.183	361.508	exp(− 610.2)
1	323.15	385.848	8.217	377.631	exp(− 588.1)	384.732	8.792	375.939	exp(− 585.5)	369.782	8.962	360.819	exp(− 561.9)
1	373.15	385.996	9.648	376.349	exp(− 507.6)	384.882	10.314	374.568	exp(− 505.2)	369.951	10.532	359.419	exp(− 484.7)
5	273.15	385.692	5.929	379.762	exp(− 699.7)	384.574	6.413	378.161	exp(− 696.8)	369.698	6.634	363.064	exp(− 668.9)
5	298.15	385.771	6.554	379.217	exp(− 640.1)	384.654	7.084	377.571	exp(− 637.3)	369.692	7.230	362.463	exp(− 611.8)
5	323.15	385.848	7.184	378.664	exp(− 589.7)	384.732	7.759	376.973	exp(− 587.1)	369.782	7.929	361.852	exp(− 563.5)
10	273.15	385.692	5.553	380.139	exp(− 700.4)	384.574	6.037	378.537	exp(− 697.4)	369.599	6.158	363.441	exp(− 669.6)
10	298.15	385.771	6.143	379.622	exp(− 640.8)	384.654	6.673	377.981	exp(− 638.0)	369.692	6.819	362.872	exp(− 612.5)
10	323.15	385.848	6.739	379.109	exp(− 590.4)	384.732	7.314	377.418	exp(− 587.8)	369.782	7.484	362.298	exp(− 564.2)

Table 2 Thermodynamic quantities ΔH_a, $T\Delta S_a$ and ΔG_a in kcal/mol and equilibrium constants, K_a, for the indicators dissociation equilibrium of phenol red, cresol red and bromophenol blue in the different solvents obtained at the B3LYP/6-31G** level of theory

	Phenol red				Cresol red				Bromophenol blue			
	ΔH_a	$T\Delta S_a$	ΔG_a	K_a	ΔH_a	$T\Delta S_a$	ΔG_a	K_a	ΔH_a	$T\Delta S_a$	ΔG_a	K_a
Ethanol	197.573	7.926	189.646	exp(− 320.1)	197.416	7.308	190.108	exp(− 320.9)	185.967	7.656	178.311	exp(− 301.1)
Water	192.192	7.686	184.506	exp(− 311.4)	192.046	7.393	184.653	exp(− 311.7)	180.903	7.788	173.115	exp(− 292.2)

Table 3 Thermodynamic quantities ΔH_a, $T\Delta S_a$ and ΔG_a in kcal/mol and equilibrium constants, K_a, for the indicators dissociation equilibrium of phenol red, cresol red and bromophenol blue with change of isotopic type of constituent atoms obtained at the B3LYP/6-31G** level of theory

	Phenol red				Cresol red				Bromophenol blue			
	ΔH_a	$T\Delta S_a$	ΔG_a	K_a	ΔH_a	$T\Delta S_a$	ΔG_a	K_a	ΔH_a	$T\Delta S_a$	ΔG_a	K_a
$^{12}C \rightarrow {}^{13}C$	385.787	7.509	378.278	exp(− 638.5)	384.670	8.039	376.631	exp(− 635.7)	369.715	8.187	361.528	exp(− 610.3)
$^{16}O \rightarrow {}^{18}O$	385.778	7.508	378.270	exp(− 638.5)	384.661	7.084	377.576	exp(− 637.3)	369.698	8.183	361.516	exp(− 610.2)
$^{1}H \rightarrow {}^{2}H$	387.909	7.891	380.018	exp(− 641.5)	386.836	7.471	379.366	exp(− 641.2)	371.755	8.580	363.176	exp(613.0)

reaction. The comparison of ΔG_a values with ΔH_a and $T\Delta S_a$ values indicates that acid ionization of indicators is controlled by entropy agent (entropy of the process) and ΔG_a values in the solvents phase are much smaller in gas phase (in view of the interactions of soluble and solvent in the CPCM model, the species become more stable, especially the pregnant species). As a result, high-polarity solvents are other favorable conditions for ionization process of indicators. In this study, all static calculations in solvents phase were carried out in Gaussian09 using density functional theory (DFT) and CPCM model as these methods are computationally efficient. However, to fully understand the origin of the ΔG_a values, a QM/MM molecular dynamic simulation study in a solvent molecular environment was used in combination with inclusion of implicit solvent, CPCM calculations, that takes into account the flexibility of the dye and the explicit interactions with the surrounding solvent molecules. This procedure allowed us to reach to a remarkable agreement between the theoretical and experimental ΔG_a values and enabled us to fully unravel the pH-sensitive behavior of sulfonphthaleine dyes in solution phase. This methodology could also be applied to other dyes and could be served as a basis for the construction of more advanced theoretical models to study the interactions of (sulfonphthaleine) dyes in a solution environment. So, it is expected in the real and experimental conditions that ΔG_a values would be smaller or they could even be negative. ΔG_a increases with isotopic change of the constituent atoms of the indicator.

The increase in ΔG_a values with isotopic change of the constituent atoms of the indicator can be interpreted by the following statistical thermodynamic relationships.

$$K_{\mathrm{C}} = \prod_i \left(\frac{q_i}{V}\right)^{\nu_i} \tag{4}$$

$$q_i = q_{\mathrm{ele}} \times q_{\mathrm{trans}} \times q_{\mathrm{rot}} \times q_{\mathrm{vib}} \times q_{\mathrm{nucl}} \tag{5}$$

$$q_{\mathrm{vib}} = \prod_j \left(\frac{\mathrm{e}^{-\theta_{\nu_j}/2T}}{1-\mathrm{e}^{-\theta_{\nu_j}/T}}\right), \quad \theta_{\nu_j} = \frac{h\nu_j}{k} \quad \text{and} \quad \nu_j = \frac{1}{2\pi}\sqrt{\frac{k_j}{\mu_j}} \tag{6}$$

The molecular partition function, q_{i}, is written as the product of electronic, q_{ele}, translational, q_{trans}, vibrational, q_{vib}, rotational, q_{rot}, and nuclear, q_{nucl}, partition functions. The vibrational partition function is given by the product of vibrational functions for each frequency. θ_{ν_j} is called the characteristic vibrational temperature and the vibrational frequencies are given by ν_j. k_j and μ_j are spring constant and reduced mass, respectively.

To this end, the molecular partition functions obtained in the frequency calculations are reported in Table 4. The obtained results show that the acidic and base forms differ greatly in the numerical values of the vibrational partition function and their differences in the other partition functions are negligible. This can be attributed to the elimination of a bond between hydrogen and oxygen atom and vibrations as to it in acidic form. When an atom in a molecule is changed to an isotope, the mass number will be changed, so μ_j will be affected but spring constant, k_j, will not (mostly). This change in the reduced mass will affect the vibrational modes of the molecule, which will affect the vibrational partition function. When an atom is replaced by an isotope of larger mass, μ_j increases leading to smaller ν_j and θ_{ν_j}. This drop in the vibrational characteristic temperature, θ_{ν_j}, increases the vibrational partition function and thereby increases the total partition function. The ratio of the numerical values of the total partition function of the isotopic state to the natural state for acidic and base forms, $q_{\mathrm{total}}(\mathrm{isotopic})/q_{\mathrm{total}}(\mathrm{natural})$, and change of the equilibrium constants with the isotopic variation of the constituent atoms of the indicators, $K_{\mathrm{a}}(\mathrm{isotopic})/K_{\mathrm{a}}(\mathrm{natural})$, are reported in Table 5. The results presented in Table 5 show that the increase in the value of the total partition function in all cases is greater for the acidic form than the base form, and this results in an equilibrium constant ratio of less than one or an increase in the ΔG_{a} by changing the constituent isotopes $\left[\Delta G_a(\mathrm{isotopic}) - \Delta G_a(\mathrm{natural}) = -RT \ln \frac{K_a(\mathrm{isotopic})}{K_a(\mathrm{natural})}\right]$. Due to $\Delta G_{\mathrm{a}} > 0$ in all states, K_{a} values are very small in all conditions. The obtained results indicate that ionization equilibrium constant was larger at high temperature and low pressure conditions and in the solution phase, especially in the polar solvents. The isotopic effect decreased K_{a} values in all cases.

Table 4 The statistical thermodynamic quantities q_{vib}, q_{trans}, q_{rot} and q_{total} calculated for a) acidic and b) base forms of phenol red, cresol red and bromophenol blue indicators in the natural state and isotopic state (with change of isotopic type of constituent atoms) obtained at the B3LYP/6-31G** level of theory

	Phenol red				Cresol red				Bromophenol blue			
	Vib	Trans	Rot	Total	Vib	Trans	Rot	Total	Vib	Trans	Rot	Total
a-natural	0.164D − 119	0.261D+9	0.114D+8	0.485D − 104	0.169D − 143	0.292D+9	0.144D+8	0.715D − 128	0.903D − 97	0.674D+9	0.555D+8	0.338D − 80
b-natural	0.185D − 113	0.260D+9	0.118D+8	0.571D − 98	0.574D − 137	0.291D+9	0.150D+8	0.251D − 121	0.237D − 90	0.672D+9	0.570D+8	0.907D − 74
a-^{13}C	0.253D − 117	0.282D+9	0.121D+8	0.864D − 102	0.443D − 141	0.317D+9	0.155D+8	0.217D − 125	0.145D − 94	0.703D+9	0.569D+8	0.581D − 78
b-^{13}C	0.279D − 111	0.281D+9	0.127D+8	0.993D − 96	0.146D − 134	0.316D+9	0.161D+8	0.746D − 119	0.370D − 88	0.701D+9	0.582D+8	0.151D − 71
a-^{13}O	0.569D − 119	0.272D+9	0.121D+8	0.187D − 103	0.596D − 143	0.304D+9	0.153D+8	0.276D − 127	0.337D − 96	0.689D+9	0.569D+8	0.132D − 79
b-^{13}O	0.636D − 113	0.271D+9	0.127D+8	0.218D − 97	0.200D − 136	0.606D+8	0.159D+8	0.192D − 121	0.875D − 90	0.687D+9	0.584D+8	0.351D − 73
a-^{2}H	0.304D − 99	0.275D+9	0.123D+8	0.103D − 83	0.531D − 117	0.312D+9	0.161D+8	0.267D − 101	0.134D − 82	0.678D+9	0.567D+8	0.522D − 66
b-^{2}H	0.641D − 95	0.273D+9	0.127D+8	0.222D − 79	0.313D − 112	0.620D+8	0.165D+8	0.321D − 97	0.752D − 78	0.684D+9	0.579D+8	0.298D − 61

*The electronic partition function in all states is equal to one

To investigate the changes in pH range of color change of indicators resulted from different physical factors (temperature, pressure, solvent and isotopic), it is assumed that the concentration ratio of $[In^-]/[HIn]$ is constant (the ratio of $[In^-]/[HIn]$ is limit ratio of the required concentrations for observation of color change of indicators.) and $[H^+]$ concentration changes in different conditions are proportional to K_a. Regarding the relationship between pH and $[H^+]$ concentration, the changes in pH of color change, ΔpH, can be calculated based on the following relationships:

$$K_{a1} = \frac{[H^+]_1[In^-]}{[HIn]} \tag{7}$$

$$K_{a2} = \frac{[H^+]_2[In^-]}{[HIn]} \tag{8}$$

$$\frac{[H^+]_2}{[H^+]_1} = \frac{K_{a2}}{K_{a1}} \tag{9}$$

$$\Delta pH = pH_2 - pH_1 \qquad pH_2 = -\log[H^+]_2 \quad \text{and} \quad pH_1 = -\log[H^+]_1 \tag{10}$$

$$\Delta pH = -\log\frac{[H^+]_2}{[H^+]_1} = -\log\frac{K_{a2}}{K_{a1}} \tag{11}$$

To study the effect of temperature on the pH of color change of the indicators, two temperature changes of 273.15 → 298.15 K and 298.15 → 323.15 K (range of each one equal to 50 K) at pressures of 1, 5, and 10 atm, and to study the effect of pressure, two pressures changes of 1 → 5 atm and 5 → 10 atm (range of each one equal to 5 atm) at temperatures of 273.15, 298.15 and 323.15 K are considered and their results are reported in Tables 6 and 7. The obtained results in Table 6 show that increasing the temperature increases the pH of color change of indicators (ΔpH > 0). This increase for each indicator is equal in the various pressures and values for phenol red, cresol red, and bromophenol blue indicators with temperature change from 273.15 K → 298.15 K were 25.884, 25.797 and 24.798, respectively, and for temperature change from 298.15 K → 323.15 K were 21.888, 21.802 and 20.976, respectively. Therefore, it can be concluded that this increase nearly is not dependent upon indicator type and pressure applied and the effect of temperature on ΔpH is lower under higher temperatures.

Table 5 The ratio of q_{total} and K_a (dissociation equilibrium constant of the indicators) in the isotopic state to the natural state for a) acidic and b) base forms of phenol red, cresol red and bromophenol blue indicators obtained at the B3LYP/6-31G** level of theory

		Phenol red			Cresol red			Bromophenol blue		
		$\frac{^{13}C}{^{12}C}$	$\frac{^{18}O}{^{16}O}$	$\frac{^{2}H}{^{1}H}$	$\frac{^{13}C}{^{12}C}$	$\frac{^{18}O}{^{16}O}$	$\frac{^{2}H}{^{1}H}$	$\frac{^{13}C}{^{12}C}$	$\frac{^{18}O}{^{16}O}$	$\frac{^{2}H}{^{1}H}$
$\frac{q_{total}(isotopic)}{q_{total}(natural)}$	a)	0.178D + 2	0.387D + 1	0.213D + 21	0.304D + 3	0.386D + 1	0.373D + 27	0.172D + 3	0.392D + 1	0.155D + 13
	b)	0.151D + 2	0.382D + 1	0.389D + 19	0.297D + 3	0.764	0.127D + 25	0.166D + 3	0.387D + 1	0.328D + 13
$\frac{K_a(isotopic)}{K_a(natural)}$		0.849	0.990	0.002	0.977	0.198	0.003	0.967	0.988	0.021

Table 6 The changes in pH of color change of indicators, ΔpH, in the gas phase resulted from change of temperature (in K) obtained at the different pressures (in atm) and the B3LYP/6-31G** level of theory

	Phenol red			Cresol red			Bromophenol blue		
	1	5	10	1	5	10	1	5	10
273.15 → 298.15	25.884	25.884	25.884	25.797	25.840	25.797	24.798	24.798	24.798
298.15 → 323.15	21.888	21.888	21.888	21.802	21.802	21.802	20.976	20.976	20.976

Table 7 The changes in pH of color change of indicators, ΔpH, in the gas phase resulted from change of pressure (in atm) obtained at the different temperatures (in K) and the B3LYP/6-31G** level of theory

	Phenol red			Cresol red			Bromophenol blue		
	273.15	298.15	323.15	273.15	298.15	323.15	273.15	298.15	323.15
1 → 5	0.697	0.695	0.695	0.695	0.695	0.695	0.695	0.695	0.695
5 → 10	0.304	0.304	0.304	0.304	0.304	0.304	0.304	0.304	0.304

Table 8 The changes in pH of color change of indicators, ΔpH, resulted from change of phase obtained at the B3LYP/6-31G** level of theory

ΔpH	Phenol red	Cresol red	Bromophenol blue
Ethanol → gas	138.279	136.716	134.240
Water → Ethanol	3.768	3.853	3.999

Table 9 The changes in pH of color change of indicators, ΔpH, in the gas phase resulted from change of isotopic type of constituent atoms obtained at the B3LYP/6-31G** level of theory

ΔpH	Phenol red	Cresol red	Bromophenol blue
$^{12}C \rightarrow {}^{13}C$	0.011	0.010	0.015
$^{16}O \rightarrow {}^{18}O$	0.005	0.703	0.078
$^{1}H \rightarrow {}^{2}H$	1.287	2.015	1.223

The results reported in Table 7 show that increasing of pressure from 1 to 5 atm for each three types of indicators at temperatures of 273.15, 298.15 and 323.15 K increased the pH of color change to the amount of 0.695, and increasing pressure from 5 to 10 atm increased the pH of color change to the amount of 0.304, and this shows that the effect of pressure on ΔpH is lower under higher pressures and is not dependent on the indicator type and temperature applied.

By considering the solvent model effect (CPCM) on the indicators, the obtained results will find more consistency with experimental samples. The results reported in Table 8 show that by changing of solvent from water to ethanol, pH of color change of the indicators, ΔpH, varies by 3.8–4.00, and by changing the phase from ethanol solvent to vacuum, ΔpH increases to about 134–138.

The isotopic effect on carbon, oxygen, and hydrogen atoms of the indicators has been studied. The results reported in Table 9 show that use of isotopes produced the increase in the pH of color change of the indicators ($\Delta pH > 0$) that their values depend on the type of atom and type of the indicator.

Conclusions

Initially, the structures of three types of sulfonphthaleine indicators including phenol red, cresol red, and bromophenol blue in modes of single anionic (acidic form) and a double anion (base form) were optimized in Gaussian 03 program package using B3LYP/6-31G** level of theory.

Vibrational frequency calculations were performed on optimized structures to ensure the stability of structures and to calculate thermodynamic values. The results from vibrational frequency calculations show that all the studied structures have real vibration frequencies or zero NIMAG.

To elucidate the effect of physical factors on the halochromic behavior of the sulfonphthaleine dyes (or change of pH of the color change of the indicators, ΔpH), acid–base equilibrium of the indicators and its related thermodynamic quantities (enthalpy change, ΔH_a, entropy change, ΔS_a, Gibbs free energy change, ΔG_a, and equilibrium constant of ionization process of indicators, K_a) are studied under different conditions; Then, their obtained values and variations are interpreted by the rules of thermodynamics and statistical thermodynamics. The obtained results indicate that the equilibrium constant of ionization is larger in the conditions of high temperatures, low pressures, polar environment and use of constructive atoms in natural state (non-use of isotopes). Therefore, it is concluded that these conditions are favorable for the reaction.

The results show that ΔpH is positive by increasing temperature at any pressure, increasing pressure at any temperature, decreasing the polarity of the solvent used and using of isotopes of constituent atoms. The effect of temperature and pressure on ΔpH is lower respectively under higher temperature and pressures and is not dependent on the indicator type. The ΔpH values due to the isotopic factor depend on the type of atom and type of the indicator.

The results of this research can help and guide the identification of favorable indicators predicting pH of their color change in different conditions. Also, these results can act as the basis for future research on the interaction of dye molecules and polymers used on fabric base. For example, using halochromic properties in the color of polymers or textiles can produce sensory materials. These textile sensors are used in the production of wound dressing. They maintain all the features of the texture, are flexible, can be used on large surfaces, and can communicate warning messages by a color change at a particular point.

References

Bamfield P (2001) Chromic phenomena, technological applications of colour chemistry, 1st edn. Cambridge, Royal Society of Chemistrys

Barachevskii VA, Kobeleva OI, Valova TM, Ait AO, Kol'tsova LS, Shienok AI, Zaichenko NL, Laptev AV, Khodonov AA, Yu Kuznetsova O, Dudinov AA, Lichitskii BV, Krayushkin MM (2012) Spectral indications of interaction of functionalized photochromic compounds with Ag and Au nanoparticles. Theor Exp Chem 48:14–20. https://doi.org/10.1007/s11237-012-9236-z

Bateman AS, Kelly SD, Jickells TD (2005) Nitrogen Isotope Relationships between crops and fertilizer: implications for using nitrogen isotope analysis as an indicator of agricultural regime. J Agr Food Chem 53:5760–5765. https://doi.org/10.1021/jf050374h

Byrne RH, Breland JA (1989) High-precision multiwavelength pH determinations in seawater using cresol red. Deep Sea Res Pt A

Oceanograph Res Pap 36:803–810. https://doi.org/10.1016/0198-0149(89)90152-0
Chang Y, Bai H, Li S, Kuo C (2011) Bromocresol green/mesoporous silica adsorbent for ammonia gas sensing via an optical sensing instrument. Sensors 11:4060–4072. https://doi.org/10.3390/s110404060
Chen W, Lin XH, Huang LY, Luo HB (2005) Electrochemical characterization of polymerized cresol red film modified glassy carbon electrode and separation of electrocatalytic responses for ascorbic. Microchim Acta 151:101–107. https://doi.org/10.1007/s00604-005-0376-x
Clayton TD, Byrne RH (1993) Spectrophotometric seawater pH measurements: total hydrogen ion concentration scale calibration of m-cresol purple and at-sea results. Deep Sea Res Pt I Oceanograp Res Pap 40:2115–2129. https://doi.org/10.1016/0967-0637(93)90048-8
Cossi M, Rega N, Scalmani G, Barone V (2003) Energies, structures, and electronic properties of molecules in solution with the C-PCM solvation model. J Comput Chem 24:669–681. https://doi.org/10.1002/jcc.10189
De Meyer T, Hemelsoet K, Van Speybroeck V, De Clerck K (2014) Substituent effects on absorption spectra of pH indicators: an experimental and computational study of sulfonphthaleine dyes. Dyes Pigm 102:241–250. https://doi.org/10.1016/j.dyepig.2013.10.048
De Meyer T, Steyaert I, Hemelsoet K, Hoogenboom R, Van Speybroeck V, De Clerck K (2016) Halochromic properties of sulfonphthaleine dyes in a textile environment: the influence of substituents. Dyes Pigm 124:249–257. https://doi.org/10.1016/j.dyepig.2015.09.007
Ensafi AA, Dadkhah-Tehrani S, Karimi-Maleh H (2010) Poly(xylenol blue) modified multiwall carbon nanotubes-glassy carbon electrode for simultaneous determination of ascorbic acid, epinephrine, and uric acid by differential pulse voltammetry. In: International Conference on Enabling science and nanotechnology, Kuala Lumpur, Malaysia. https://doi.org/10.1109/ESCINANO.2010.5700983
Flores R (1978) A rapid and reproducible assay for quantitative estimation of proteins using bromophenol blue. Anal Biochem 88:605–611. https://doi.org/10.1016/0003-2697(78)90462-1
Frisch MJ et al (2004) Gaussian 03, Revision C.02. Gaussian, Inc., Wallingford
Gibson LT, Ewlad-Ahmed A, Knight B, Horie V, Mitchell G, Robertson CJ (2012) Measurement of volatile organic compounds emitted in libraries and archives: an inferential indicator of paper decay. Chem Cent J 6:42. https://journal.chemistrycentral.com/content/6/1/42
Ghanadzadeh Gilani A, Taghvaei V, Moradi Rufchahi E, Mirzaei M (2017) Photo-physical and structural studies of some synthesized arylazoquinoline dyes. Spectrochim Acta A 185:111–124. https://doi.org/10.1016/j.saa.2017.05.035
Golchoubian H, Mehrbanian D, Rezaee E, Xu ZX (2019) Structural and chromotropism properties of copper(II) complexes with 3,3′-((pyridin-2-ylmethyl)azanediyl)dipropanamide ligand. Transit Metal Chem 44:671–680
Hermosilla L, Caroli Rezende M, Gageiro Machado V, Stock RI (2017) Thermohalochromism of phenolate dyes conjugated with nitro-substituted aryl groups. Spectrochim Acta A 173:556–561. https://doi.org/10.1016/j.saa.2016.10.017
Hosseini M, Heydari R, Alimoradi M (2014) A novel pH optical sensor using methyl orange based on triacetylcellulose membranes as support. Spectrochim Acta A 128:864–867. https://doi.org/10.1016/j.saa.2014.02.171
Hua X, Hou X, Gong X, Shen G (2013) Electrochemical behaviour of 5-fluorouracil on glassy carbon electrode modified with bromothymol blue and multiwalled carbon nanotubes. Anal Methods 5:2470–2476
Kelly FM, Cochrane C (2015) Color-changing textiles and electrochromism. In: Tao X (ed) Handbook of smart textiles. Springer, Singapore, pp 859–889. https://doi.org/10.1007/978-981-4451-45-1_16
Kim S (2006) Functional dyes. Elsevier, Amsterdam
Kulinich AV, Ishchenko AA (2019) Structures and fluorescence spectra of merocyanine dyes in polymer films. J App Spectrosc 86:35–42. https://doi.org/10.1007/s10812-019-00777-6
Kulinich AV, Ishchenko AA, Bondarev SL, Sukhodola AA (2018) Effect of temperature on the spectral fluorescent properties of positively solvatochromic merocyanines. Theor Exp Chem 54:331–338. https://doi.org/10.1007/s11237-018-9578-2
Kurzweilová H, Sigler K (1993) Fluorescent staining with bromocresol purple: a rapid method for determining yeast cell dead count developed as an assay of killer toxin activity. Yeast 9:1207–1211. https://doi.org/10.1002/yea.320091107
Marona H, Schapoval E (2001) Spectrophotometric determination of sparfloxacin in pharmaceutical formulations using bromothymol blue. J Pharm Biomed Anal 26:501–504. https://doi.org/10.1016/s0731-7085(01)00429-0
Matějec V, Barton I, Pospisilova M, Traplova L (2019) Extrinsic fiber-optic sensor for detection of saliva pH. Chem Afr 2:301–307. https://doi.org/10.1007/s42250-019-00050-5
Mineo PG, Vento F, Abbadessa A, Scamporrino E, Nicosia A (2019) An optical sensor of acidity in fuels based on a porphyrin derivative. Dyes Pigm 161:147–154. https://doi.org/10.1016/j.dyepig.2018.09.045
Nakamura N, Amao Y (2003) An optical sensor for CO_2 using thymol blue and europium (III) complex composite film. Sens Actuators B 92:98–101. https://doi.org/10.1016/S0925-4005(03)00098-4
Özyiğitoğlu G (2020) use of Lichens in biological monitoring of air quality. Environ Concerns Sust Develop. https://doi.org/10.1007/978-981-13-5889-0_3
Steyaert I, Rahier H, De Clerck K (2015) Nanofibre-based sensors for visual and optical monitoring. NanoSci Technol 96:157–177. https://doi.org/10.1007/978-3-319-14406-1_7
Sun X, Branford-White C, Yu ZW, Zhu LM (2015) Development of universal pH sensors based on textiles. J Solgel Sci Technol 74:641–649. https://doi.org/10.1007/s10971-015-3643-2
Surati PR, Shah BA (2015) Photochromic and molecular switching behaviour of Schiff base-containing pyrazolone ring. Chem Pap 69:368–375. https://doi.org/10.1515/chempap-2015-0021
Tomasi J, Persico M (1994) Molecular interactions in solution: an overview of methods based on continuous distributions of the solvent. Chem Rev 94:2027–2094. https://doi.org/10.1021/cr00031a013
Van der Schueren L, Hemelsoet K, Van Speybroeck V, De Clerck K (2012) The influence of a polyamide matrix on the halochromic behaviour of the pH-sensitive azo dye Nitrazine Yellow. Dyes Pigm 94:443–451. https://doi.org/10.1016/j.dyepig.2012.02.013
Yang G, Yan J, Qi F, Sun C (2010) High Sensitivity and Reproducibility of a Bismuth/Poly(bromocresol purple) film modified glassy carbon electrode for determination of trace amount of cadmium by differential pulse anodic stripping voltammetry. Electroanal 22:2729–2738. https://doi.org/10.1002/elan.201000260

Yao W, Byrne R (2001) Spectrophotometric determination of freshwater pH using bromocresol purple and phenol red. Environ Sci Technol 35:1197–1201. https://doi.org/10.1021/es001573e

Zhang L, Li Z, Chang R, Chen Y, Zhang W (2009) Synthesis and characterization of novel phenolphthalein immobilized halochromic fiber. React Funct Polym 69:234–239. https://doi.org/10.1016/j.reactfunctpolym.2009.01.001

Zollinger H (2003) Color chemistry: synthesis, properties, and applications of organic dyes and pigments. VHCA en, WILEY-VCH

Publisher's Note Springer Nature remains neutral with regard to jurisdictional claims in published maps and institutional affiliations.